Multi-Objective Optimization of Mitigation Strategies for Buildings Subject to Multiple Hazards

Himadri Sen Gupta¹, Tarun Adluri¹, Dylan Sanderson², Andrés D. González¹, Charles D. Nicholson¹, Daniel Cox²

4

5

6

3

1

2

¹School of Industrial and Systems Engineering, University of Oklahoma, Norman, OK 73019, USA

² School of Civil and Construction Engineering, Oregon State University, Corvallis, OR, 97330, USA

7

9

10

11

12

13

14

15

16

17

18

19

20

21

22

23

24

25

26

27

8 Abstract

Natural hazards can have a devastating impact on communities, leading to social and economic losses. These effects are particularly severe in multi-hazard contexts, where multiple disruptive events occur simultaneously or consecutively (such as earthquakes and tsunamis). To reduce the impact of such events, it is critical to enhance community resilience and make it more capable of withstanding and recovering from diverse types of damage. In this study, we propose a multi-objective optimization model to determine optimal retrofitting strategies to enhance community resilience under multiple hazards. We used the proposed model to analyze the impact of earthquake and tsunami hazards on the community of Seaside, Oregon. It assesses the effectiveness of different retrofitting strategies at the parcel scale, considering the conflicting objectives of reducing overall economic loss, population dislocation, and building repair times. Our results demonstrate that retrofitting buildings to achieve higher seismic codes can significantly reduce the impact of natural hazards on structural damage, population dislocation, and building repair times. Additionally, our findings reveal the importance of considering geographical location and mitigation measures when optimizing retrofitting strategies. By considering budget constraints and community resilience metrics, our model identifies the most effective retrofitting strategies for individual buildings of Seaside, which ultimately helps the community make informed decisions about investments to reduce the impact of natural hazards. Overall, this study provides valuable insights into the importance of enhancing community resilience in multi-hazard contexts and showcases the use of a multiobjective optimization model to identify optimal retrofitting strategies.

Keywords: Multi-hazard; multi-objective optimization; community resilience; building mitigation; population dislocation.

28

29

30

31

1. Introduction

Community structures, transportation, communication, and power systems across a community or geographic area, the economy, and the accessibility to social services can all suffer severe harm and disruptions due to natural and human-

caused hazards [1-3]. Additionally, the social capital of a community, which refers to the networks and relationships that enable effective response and recovery, can also be affected by these hazards [4–8]. Therefore, it is crucial to seek effective ways to improve the resilience of communities and their structures against such hazards. The impact that these hazards have on communities can be devastating. Natural hazards threaten life safety, and damage to infrastructure can disrupt communities. The effects of which can last years following the initial event [9,10]. In light of these hazards, mitigation strategies that reduce the damage can be employed. These depend on various elements, such as risks, time and budgetary constraints [11], and community values. Retrofitting structures as a mitigation method against flooding, earthquakes, and tornadoes involves adjusting existing buildings to withstand these hazards better. On the other hand, mitigating the effects of tsunamis involves relocating structures from tsunami inundation zones and strengthening buildings to resist the forces of tsunamis [12].

To improve a community's ability to respond to hazards, the field of resilience planning has gained traction. This area of study aims to both quantify and reduce the negative impacts of hazards on communities [13-16]. The concept of resilience, which was first applied to communities in the context of natural hazards by Bruneau et al. (2003), refers to a community's ability to adapt and sustain operations during hazardous events [17]. The study of community resilience is interdisciplinary, involving fields such as ecology, psychology, and economics. As a result, resilience planning should consider the natural, built, and socioeconomic environments [18-22]. Despite ongoing research in various disciplines, the integration of all elements of community resilience is still lacking. For example, Guidotti et al. (2019) studied population dislocation and the ability of a water network to meet demand, while Franchin & Cavalieri (2015) looked at population dislocation and road damage using a Bayesian network [23,24]. Additionally, Kavvada et al. (2022) presented a novel model, contemplating the dual aspects of economic and environmental implications of earthquake retrofitting. Using San Francisco as a reference, it also highlights an original method for equitable resource distribution, underlining the importance of balancing economic prudence and social fairness in disaster readiness [25]. While this study focuses on retrofitting strategies for buildings, it is important to acknowledge that social capital also plays a role in overall community resilience. It encompasses trust, cooperation, and shared norms within a community, which can significantly contribute to quicker recovery and better adaptation post-disaster. Hence, although our focus is on structural mitigation measures, the interplay between physical infrastructure and social resources should not be overlooked [26–33].

Decision support systems for natural hazards aim to lower risks and/or boost community resilience. A comprehensive review of decision support systems for natural hazards [34] evaluated more than a hundred papers and devised a decision support system classification system. According to Newman et al. (2017), decision support systems can relate to (i) exploring risks associated with natural hazards under present-day conditions [2,35], (ii) manually evaluating risk-reduction alternatives via what-if scenarios [35], and (iii) developing models that determine optimal solutions and automatically develop risk reduction plans [36,37]. Each of these, according to Newman et al. (2017), exhibits increasing levels of decision support [34]. This study indicates that the field of decision support systems has concentrated chiefly on the first two domains, evaluating risk and resilience, but less work has been concentrated on optimizing mitigation measures,

despite this areas rising popularity.

32

33

34

35

36

37

38

39

40

41

42

43

44

45

46

47

48

49

50

51

52

53

54

55

56

57

58

59

60

61

62

63

64

65

66

67

68

Within this subdiscipline of decision support systems applied to natural hazards, optimization can relate to either preemptive mitigation or restoration strategies. Considering the former, Zhang and Nicholson (2016) developed a multiobjective optimization model considering the performance of interdependent physical, social, and economic systems under disruption from earthquake hazards [38], and Wen (2021) extended that work by implementing new objectives to the optimization model which was applied for tornado hazard [39]. Through this work, Wen (2021) suggested mitigation measures for building blocks under tornado hazard and, after that, Gupta et al. (2022) formulated an optimization model for building-level mitigation measures for the community under flooding hazard [40]. On the other hand, considering the optimization of restoration strategies, González et al. (2016) and Gomez et al. (2019) posed the Interdependent Network Design Problem (INDP), which is concerned with determining the least-cost reconstruction strategy for a partially destroyed system of interdependent infrastructure networks [37,41]. Similarly, Zhang, Wang, and Nicholson (2017) considered the post-disaster recovery of road and bridge transportation networks [42].

Given that communities are often prone to multiple hazards, this paper presents an optimization model for enhancing the community's resilience against multiple natural hazards. Namely, a multi-objective optimization model for building mitigation strategies subject to multiple hazards is proposed. While multi-objective optimization models for resilience have been developed by Zhang and Nicholson (2016), Wen (2021), and Gupta et al. (2022), the novelty of this paper lies in that multiple hazards are considered, and the solutions provided are the individual building level [38,39,43]. As such, mitigation options that target either both or one of the underlying hazards are included in the model. Further, the multi-objective aspect of this framework provides avenues to consider the impact that hazards have on buildings and the population, which was previously not considered by Gupta et al. (2022) [40]. The remainder of this paper is organized as follows. The approach and formulation of the multi-objective optimization model are covered in Section 2 of the remaining text. The suggested model is applied to Seaside, Oregon, as a case study in Section 3; the results are then discussed, and conclusions are presented in Section 4. Section 4 also covers future research directions.

2. Research Methodology

The multi-objective optimization of building mitigation strategies subject to multiple hazards is shown in **Figure 1**. This model assumes a community with one or more distinct zones. A community zone is any defined geographic region that contains structures of interest. Such zones could be based on census tracts, topographically distinct regions, or areas of relative homogeneity in structure types or purposes. Furthermore, it is believed that the community has information related to structure type, retail market value, and the population at the parcel level. The framework consists of four primary steps: (i) defining decision support options, (ii) performing the multi-hazard damage analysis, (iii) extracting metrics from the multi-hazard damage analysis to be used in the optimization model, and (iv) performing the multi-objective optimization. The following subsections outline each of these steps in detail.

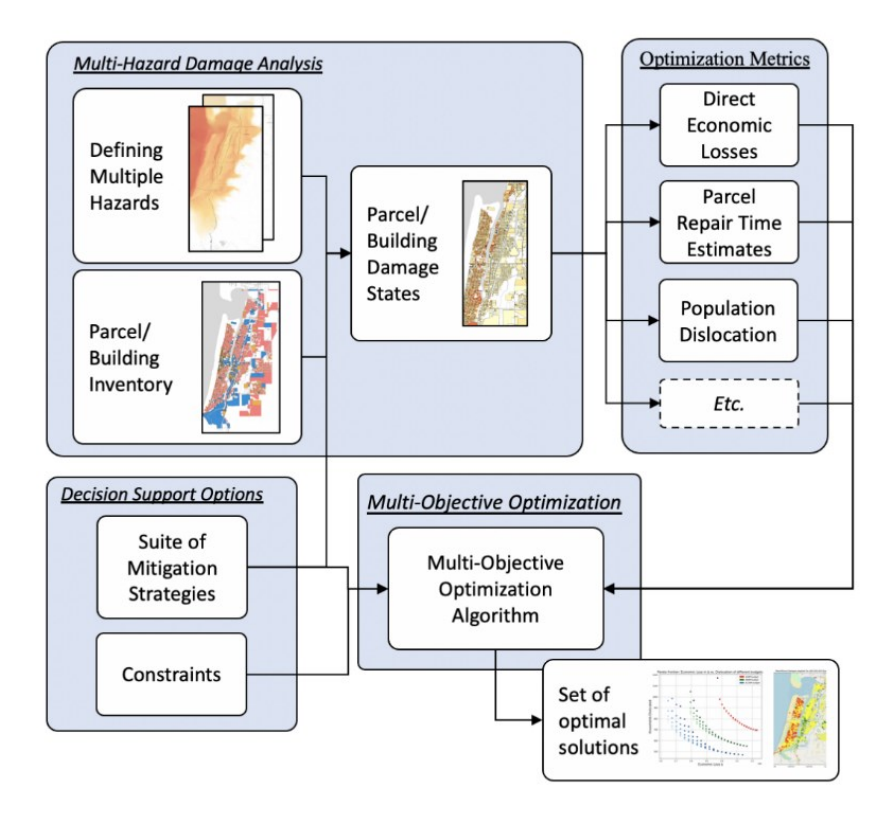


Figure 1: Framework demonstrating the detailed research methodology.

2.1. Decision Support Options

The first step in this framework is to define decision support options, which consists of identifying: (i) a suite of mitigation strategies to consider and (ii) constraints that are employed in the optimization model. In the context of disasters, the former can consist of either proactive or reactive strategies. The costs of implementing each of the mitigation strategies should be defined. The latter consists of identifying constraints that are employed in the optimization model and can consist of items such as budgetary or resource limits.

2.2. Multi-Hazard Damage Analysis

Following the identification of decision support options, a multi-hazard damage analysis is performed to determine the probability of being in a certain damage state for each parcel. This step involves mapping spatially explicit hazard intensity measures of the underlying individual hazards to the built environment. This is shown in **Figure 1** via the connections between the multiple hazards and the parcel/building inventory box. Methods to employ a multi-hazard damage analysis are numerous and can range from using fragility surfaces to assuming the underlying hazards and damages are statistically independent [44,45]. For a comprehensive review of multi-hazard risk and damage analyses, readers are directed to [2].

2.3. Optimization Model Parameters

One of the key components in constructing an optimization model is the model parameters, which have a significant impact on the optimization results. In this case, the required parameters are obtained from a multi-hazard damage

analysis. The important parameters of this multi-objective optimization model include the predicted direct economic loss due to building damage, the expected displacement of the population due to natural hazards, and the estimated repair time required to address disaster damage. Let, l_{ik} denote the expected direct economic loss due to a multi-hazard scenario for building in parcel $i \in \mathcal{Z}$ and mitigation option $k \in \mathcal{K}$. These mitigation measures for buildings for various natural hazards refer to actions or strategies that aim to reduce the negative impacts of these hazards on the built environment. These measures can include physical modifications to buildings and infrastructure, such as retrofitting or reinforcing structures to better withstand specific hazards, as well as non-structural measures, such as land-use planning, early warning systems, and emergency management plans [46]. The calculation of direct economic loss due to building damage is presented in equation (1).

$$l_{ik} = v_{ik} \left(\sum_{ds} P_{ds} * r_{ds} \right) \tag{1}$$

In equation (1), v_{ik} is the retail market value (also known as appraisal value) of the building in parcel $i \in \mathcal{Z}$ and mitigation option $k \in \mathcal{K}$, r_{ds} is the damage ratio associated with the damage state(ds) of the building in parcel $i \in \mathcal{Z}$ and mitigation option $k \in \mathcal{K}$. For this study, four damage state probabilities are considered and each of it has a damage factor depending on a hazard. Probability of damage state is presented by P_{ds} in the equation.

The damage state probabilities are additionally used for the calculation of population dislocation which is the second community resilience metric in our research, was computed by Rosenheim et al. [47]. The human systems response, household dislocation, was modeled using data and results from housing unit and household surveys conducted in the aftermath of Hurricane Andrew based on the loss of property value; the model forecasts the likelihood of household dislocation. Let d_{ik} be the expected population dislocation due to a multi-hazard scenario for building in parcel $i \in \mathcal{Z}$ and mitigation option $k \in \mathcal{K}$. The dislocation is computed from four dislocation probabilities based on a random beta distribution of the four damage factors provided by Bai et al. [48] . These four damage factors correlate to a loss of value. The likelihood of dislocation is calculated as the sum of the four probabilities multiplied by the four probabilities of damage states. In the research article by Rosenheim et al. (2019), the authors aim to calculate the population dislocation due to the impact of natural hazards on buildings [47]. To do this, they use a logistic regression equation (Equation 2) that considers the probability of dislocation [49] for each building, denoted by p_{ik}^d . The equation includes various parameters that affect the probability of dislocation, such as the expected direct economic loss due to building damage (p_{ik}^{loss}), the a binary variable (d_k^{sf}), representing single family home (1) or not (0). and the percentage of African American residents in block group (p_k^{black}). Additionally, the equation also includes the parameter p_k^{hisp} which represents percent Hispanic residents in block group.

$$p_{ik}^{d} = \frac{1}{1 + e^{-\left(b_0 + b_1 p_{ik}^{loss} + b_2 d_k^{sf} + b_3 p_k^{black} + b_4 p_k^{hisp}\right)}}$$
(2)

Once the probability of dislocation is calculated, the authors then multiply it with the number of people living in each building at parcel n_{ik} to determine the expected value of population dislocation, d_{ik} . This expected value provides an estimate of the number of people who may be dislocated due to the impact of natural hazards on the building at parcel n_{ik} for $i \in \mathcal{Z}$ and mitigation option $k \in \mathcal{K}$, given in equation (3).

$$d_{ik} = p_{ik}^d * n_{ik} \tag{3}$$

The final community resilience metric is the amount of time it will take to repair each building. HAZUS provides median repair time estimates for each building type and damage state. Here it is assumed that the four damage states, none/insignificant, moderate, heavy, and complete, have median repair times of 0.5, 60, 360, and 720 days, respectively. Following Kameshwar et al. (2019), it is assumed that these median repair time estimates correspond to a lognormal distribution, each with a dispersion of 0.5 [35]. The mean associated with each lognormal repair time curve is determined (u_{rds}) , and the expected repair time at each parcel is computed as in equation (4) and (5).

$$R_{ik} = \sum_{ds} P_{ds} * u_{rds} \tag{4}$$

155 The average repair time of the community will be,

$$t_{ik} = \frac{R_{ik}}{\sum b_{ik}} \tag{5}$$

2.4. Multi-Objective Optimization Model

To define the optimization problem, let \mathcal{Z} denote the set of parcels and \mathcal{K} denote the set of mitigation options. The decision variable gives the information of total number of buildings in parcel and mitigation option and the second decision variable gives the information of total number of buildings retrofitted from mitigation option to mitigation option, in parcel. Assuming that no mitigation option is applied to the building at the beginning, we assume that the buildings are initially at mitigation option k=0. The model determines the quantities of each building to be retrofitted with which mitigation option.

Once, we have calculated these three metrics/parameters at the parcel level; we convert the information to the community level by multiplying the number of buildings in each parcel. The number of buildings in each parcel $i \in \mathcal{Z}$ and mitigation option $k \in \mathcal{K}$ can be defined as b_{ik} .

The expected economic loss, population dislocation and repair time of the community is given by equation (6), (7), and (8), respectively,

$$\sum_{i\in\mathcal{I}}\sum_{k\in\mathcal{K}}l_{ik}b_{ik}\tag{6}$$

$$\sum_{i\in\mathcal{I}}\sum_{k\in\mathcal{K}}d_{ik}b_{ik}\tag{7}$$

$$\sum_{i\in\mathcal{I}}\sum_{k\in\mathcal{K}}t_{ik}b_{ik}\tag{8}$$

Since we want to study the effects of modifying the buildings using diverse mitigation options, we incorporate a decision variable x_{ik} , defined as the number of buildings in each parcel $i \in \mathcal{Z}$ and mitigation option $k \in \mathcal{K}$ after the strategy/policy mitigation actions have been implemented. Thus, the mitigation strategy/policy used on the community would result in the difference between x_{ik} and b_{ik} . Thereby, the objective functions for the model can be calculated by simply be replacing b_{ik} with x_{ik} from the equations (6), (7), (8) and adding whether we want to minimize or maximize the metrics. In this case these metrics need to be minimized to reach optimum values, as the goal is to reduce economic loss, population dislocation, and repair time. The objective functions of the proposed optimization model are as shown in equations (9) – (11).

$$min\sum_{i\in\mathcal{I}}\sum_{k\in\mathcal{K}}l_{ik}x_{ik} \tag{9}$$

$$\min \sum_{i \in \mathcal{I}} \sum_{k \in \mathcal{K}} d_{ik} x_{ik} \tag{10}$$

$$\min \sum_{i \in \mathcal{I}} \sum_{k \in \mathcal{K}} t_{ik} x_{ik} \tag{11}$$

Although the current model, we are presenting minimization of economic loss, population dislocation, and building repair time within the community as example, it is designed to be generalizable to accommodate other key metrics, both economic and socio physical. For instance, the objective function could be extended to encompass factors such as possible

impact of social capital or building functionality [39,50] in the context of natural hazard vulnerability. In this modified scenario, metrics like 'expected economic losses' could be replaced or complemented by 'social capital vulnerability' or 'level of post-disaster building functionality' as objectives to be optimized. More generally, the model can be adapted for a multi-objective setting, where the aim is to simultaneously maximize or minimize multiple social metrics (as depicted in Equation 12). This can be accomplished through the formulation of a set of objective functions, denoted as $n \in N$, where ψ^n_{ik} represents the expected value of the chosen metrics (e.g., economic loss, population dislocation, contribution of social capital, building functionality etc.) for each building $i \in Z$, subjected to the mitigation strategy $k \in K$.

minimize or maximize
$$\sum_{i\in\mathbb{Z}}\sum_{k\in\mathcal{K}}\psi_{ik}^{n}x_{ik}, \quad \forall n\in\mathbb{N}$$
 (12)

The optimization approach, in turn, strategically allocates scarce resources to retrofit as many buildings as possible by mitigation options while simultaneously attempting to mitigate direct loss, population dislocation, and repair time at the community level. The other decision variable will help here, $y_{ijkk'}$ denotes the total number of buildings $i \in Z$, of archetype $j \in S$, associated with retrofit strategy level $k \in K$ to level $k' \in K$. As a result, for each mitigation option, the model determines the number of buildings that would need to be modified for other mitigation measures. Given the scarcity of resources to retrofit the buildings, it is considered that we have a total maximum budget of B. The cost of improving from mitigation option $k \in \mathcal{K}$ to mitigation option $k' \in \mathcal{K}$, in parcel $i \in \mathcal{Z}$ is $c_{ikk'}$. The optimization model is informed with the constraint (13) to maintain the retrofit building to be below the total available budget.

$$\sum_{i \in \mathcal{I}} \sum_{k \in \mathcal{K}} \sum_{k' \in \mathcal{K}} c_{ikk'} y_{ikk'} \le B \tag{13}$$

Another set of constraints is making sure that the total number of buildings after retrofitting from mitigation option $k \in \mathcal{X}$ to mitigation option $k' \in \mathcal{K}$ in parcel $i \in \mathcal{Z}$ is equal to the total number of buildings before retrofitting, which is presented by constraints (14).

$$x_{ik} = \sum_{k':(k',k)\in\mathcal{L}} y_{ik'k} + b_{ik} - \sum_{k':(k,k')\in\mathcal{L}} y_{ikk'} \ \forall i \in \mathcal{Z}, \forall k \in \mathcal{K}$$

$$\tag{14}$$

Constraints (15) to maintain a balance in the number of buildings in each parcel $i \in \mathcal{Z}$ before and after retrofitting.

$$\sum_{k \in \mathcal{K}} x_{ik} = \sum_{k \in \mathcal{K}} b_{ik}, \qquad \forall i \in \mathcal{Z}$$
 (15)

Finally, the last set of constraints (16) and (17) are to present the domain of the decision variables which are non-negative integer variables.

$$x_{ik} \in \mathbb{Z}^{\geq 0}, \quad \forall i \in \mathcal{Z}, k \in \mathcal{K}$$
 (16)

$$y_{ikk'} \in \mathbb{Z}^{\geq 0}, \quad \forall i \in \mathcal{Z}, (k, k') \in \mathcal{L}$$
 (17)

3. Case Study: Application to Seaside, Oregon

The present study delves into the impact of a multi-hazard scenario in Seaside, Oregon, which is a vulnerable coastal community located in the North American Pacific Northwest. The region is prone to the rupture of the Cascadia Subduction Zone (CSZ), a significant 1,000 km fault line stretching from Cape Mendocino to Vancouver Island, and is formed by the convergence of Juan de Fuca, Explorer, and Gorda plates beneath the North American Plate [51]. This rupture can result in a catastrophic earthquake and tsunami, and Seaside, with its high social vulnerability index, has been estimated to have 87% of its developed land within the inundation zone [52]. Therefore, Seaside was selected as the testbed community for this study, and it has been the focus of numerous other studies, owing to its susceptibility to the CSZ [23,35,45,47,53–56]. The city and its location, along with its building attributes, are illustrated in Figure 2, providing a comprehensive picture of the region's exposure to the multi-hazard scenario. In addition to the attributes shown in Figure 2, each building's structural value is available.

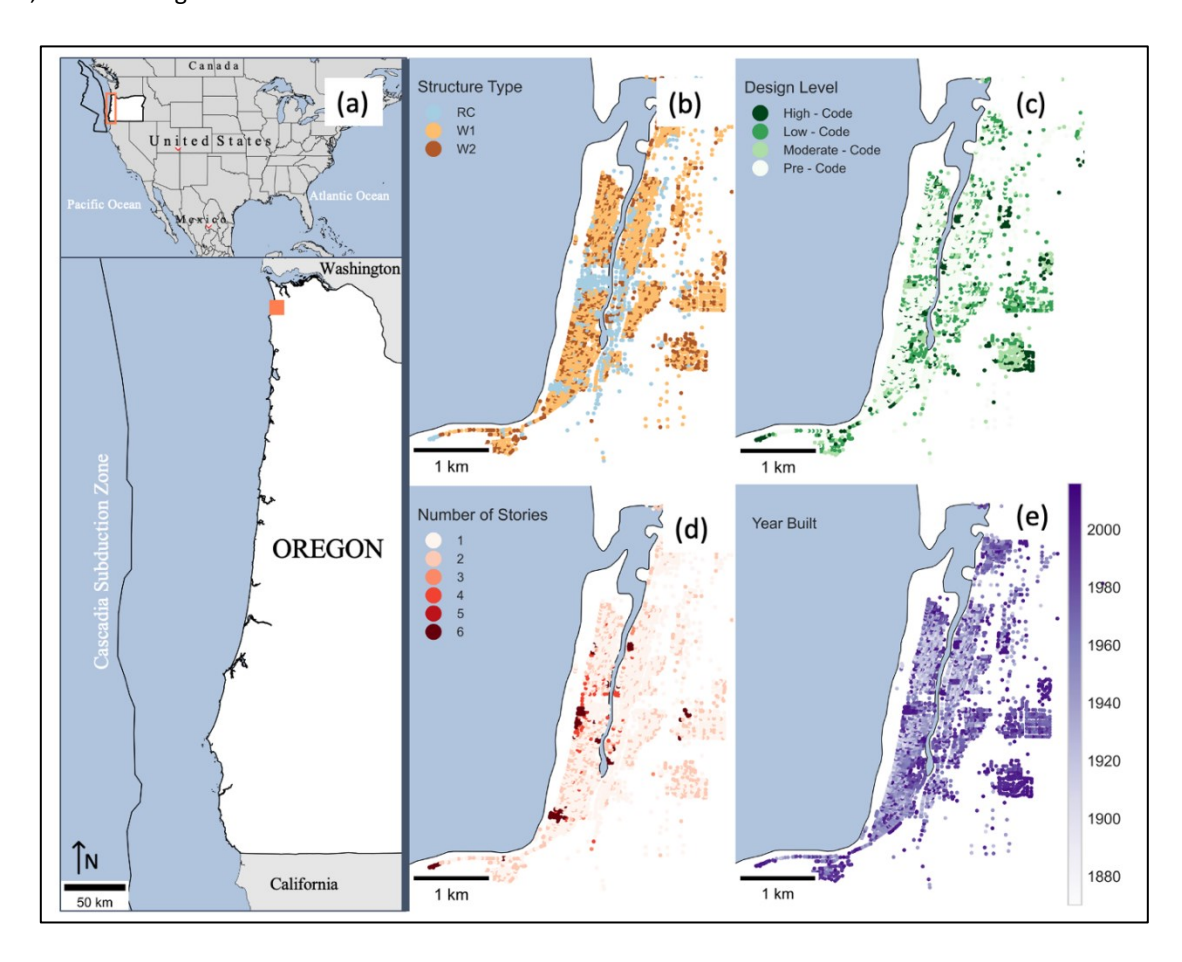


Figure 2: A overview of the location of Seaside in United States map (a) and locations of buildings based of various building archetypes (b), current design level (c), number of stories (d), year build (e) of each individual building.

The objectives of this optimization model can be determined by selecting any metric that reflects some dimension of performance (or resilience) of the community in question. The selected metric must be readily available at the building level. For the purpose of this study, the objectives are based on the scenario in Seaside, Oregon. As reported by Wiebe and Cox (2014), the economic losses from building damage in Seaside, Oregon after a catastrophe can reach a staggering \$1.2 billion. This estimate was obtained by utilizing a methodology for calculating building damage at a community level using fragility curves [57]. A fragility curve is a statistical function that reflects the performance (or damage state) of a given demand. It is typically shaped like an "S" and embodies the uncertainty in the system's ability to withstand a specific loading condition [58]. Fragility curves can be created through judgmental, empirical, analytical, or hybrid methods [58]. In the case of tsunamis, fragility curves have historically been established empirically through field observations, laboratory experiments, and numerical simulations. In this paper, the advantage of using fragility curves is that it allows for the integration of all risks and uncertainties into a single function [57]. This methodology enables the calculation of damage at the individual building level. In this research, only the direct tangible economic loss, represented by building damage, was considered. It is important to note that although direct intangible losses, such as death, and indirect tangible losses are also critical factors in disaster scenarios, they were not taken into account in this study. Nevertheless, the largest economic losses from hazards like earthquake or tsunami are still sustained by buildings and their contents.

This work employs the results of a Probabilistic Seismic and Tsunami Hazard Analysis (PSTHA) carried out by Park, Cox, and Barbosa (2017). The PSTHA consisted of defining earthquake fault source models and characteristics, creating a logic tree for a full-margin rupture of the CSZ, and computing earthquake and tsunami intensity measures. The PSTHA ultimately resulted in earthquake and tsunami hazard layers for seven different recurrence intervals, including 100, 250, 500, 1000, 2500, 5000, and 10,000-year. Parcel-level data that was initially collected to demonstrate a probabilistic tsunami damage analysis is used here to represent the building inventory [53,59]40] Building losses are measured in pylncore by overlaying hazard maps on the structures and assessing site-specific severity measures [60–62]. Pylncore enables users to access, automate, and analyze various hazard-related data and risk models using Python [63]. With pylncore, researchers and decision-makers can run risk assessments, execute hazard models, and create custom workflows for comprehensive risk analysis and mitigation. For the earthquake and tsunami, intensity indices of spectral displacement and momentum flux are used [35]. Previous studies have shown that the 500-year and 1000-year events presented the most significant economic risk [55]. In this study we consider these two recurrence intervals for the multi-objective optimization.

In this work, Interdependent Networked Community Resilience Modeling Environment (IN-CORE), an open-source community resilience modeling environment, is used to perform structural damage analysis [64]. HAZUS fragility models were used to determine the probability of being in or exceeding a given damage state [44,65] and are characterized by a lognormal distribution given in Equation (18).

$$P[ds|D] = \Phi\left[\frac{1}{\beta_{ds}}ln\left(\frac{D}{\overline{D}_{ds}}\right)\right]$$
(18)

250 251

252

253 254

256

257

258

259

260

261

262

263

264

265

Where ds is the damage state, D is the demand on the structure, eta_{ds} is the lognormal standard deviation, and \overline{D}_{ds} is the median of the lognormal distribution associated with damage state ds. This parameterization of lognormal distributions is used for both the earthquake and tsunami fragility curves. For earthquake hazards, spectral displacement is employed as the demand type, whereas momentum flux is employed for the tsunami hazard.

The lognormal fragility parameterization depends on the structure type and seismic code. As previously mentioned, mitigation option 1 corresponds to retrofitting the structure to the highest seismic code, thus shifting the seismic fragility curves. Example fragility curves for a reinforced concrete structure under high seismic code is illustrated in Figure 3.

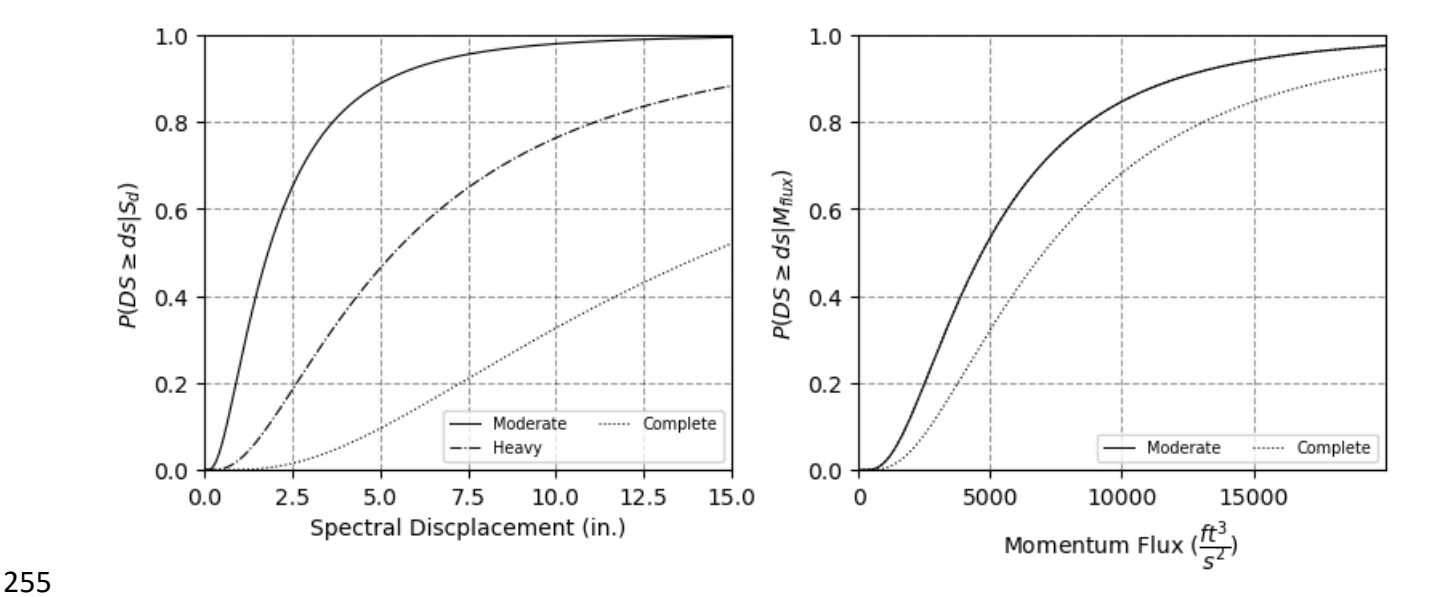


Figure 3: Example fragility curves for a reinforced concrete structure under high seismic code.

Moreover, pylncore uses three limit states and four damage states (none/insignificant, moderate (M), heavy (H), and complete (C)). Specific definitions of damage vary by structure type, but can generally be defined as follows: moderate damage corresponds to small cracks in shear walls or beams and columns; extensive damage corresponds to large cracks, frame elements have their reached capacity, and braces have failed; complete damage corresponds to significant portion of structural elements have exceeded capacities or the structure has collapsed. The single hazard analysis results in the probability of being in each of the four damage states for both earthquake and tsunami hazards as well as provide limit state probabilities. A cumulative building damage module in pylncore combines the damage and limit state probabilities of individual hazards to cumulative damage/limit state probabilities assuming statistical independence [62]. The cumulative limit state probabilities considering both the earthquake and tsunami hazards are given in equations (19-21).

$$P_{comb}[DS = C] = P[DS = C|Eqke] + P[DS = C|Tsu] - P[DS = C|Eqke] \cdot P[DS = C|Tsu]$$

$$+ (P[DS \ge H|Eqke] - P[DS = C|Eqke]) \cdot (P[DS \ge H|Tsu] - P[DS = C|Tsu])$$
(19)

$$P_{comb}[DS \ge H] = P[DS \ge H|Eqke] + P[DS \ge H|Tsu] - P[DS \ge H|Eqke] \cdot P[DS \ge H|Tsu]$$

$$+ (P[DS \ge M|Eqke] - P[DS \ge H|Eqke]) \cdot (P[DS \ge M|Tsu] - P[DS \ge H|Tsu])$$
(20)

The Seaside community comprises of 4,453 buildings and a population of 6,457 individuals. The overall real market value of these buildings amounts to an estimated \$829,171,004. Based on the calculations, there is a potential for 25% direct loss due to a 500-year event and 50% direct loss due to a 1000-year event. The direct economic losses are computed using damage ratios and each parcel's actual market value. Here it is assumed that the four damage states of none/insignificant, moderate, heavy, and complete have damage ratios of 0.005, 0.155, 0.55, and 0.90, respectively. The expected economic loss is a function of the retail market value of the building and the probability of being in a damaged state which is considering various mitigation measures. For calculating the expected population dislocation, we needed to use Equations (2) and (3). In equation (2), the following parameters are used: $b_0 = -0.42523$, $b_1 = 0.02480$, $b_2 = -0.50166$, $b_3 = -0.01826$, and $b_4 = -0.01198$. It should be noted that the default values of these parameters were developed for the MAEViz earthquake model (Lin et al., 2008) and have been used in previous studies for Seaside considering earthquake damage (Rosenheim et al., 2021). We assume that the parameters in equation (2) can be used as-is because the description of damage states for earthquake and tsunami damage are the same.

Unfortunately, the estimated repair times greatly exceed the target recovery time outlined by the Oregon Seismic Safety Policy Advisory Commission (OSSPAC) [66]. Moreover, it is estimated that in the event of these hazards, 40-50% of the population may experience dislocation.

Table 1: Community metrics with no mitigation strategy

Return Period (Years)	Economic Loss (Million)	Population Dislocation	Average Repair Time (Days)
500	\$237	2574	220
1000	\$405	3157	455

The multi-objective optimization paradigm is applied to Seaside in the sections below, which also show mitigation tactics for the multiple-hazard earthquake tsunami linked to the CSZ. The following sections are arranged per the flowchart in **Figure 1**. The first step consists of defining the decision support options. For the case study, community metrics with no mitigation strategy are given in Table 1 and four mitigation strategies are considered which are summarized in Table 2. The mitigation options outlined herein are employed to demonstrate the multi-objective optimization framework applied to multiple hazards. Costs associated with each strategy are not exact and can be refined in future work. All parcels are initially considered under status quo conditions (Option 0). Park et al. (2017) classified the buildings into HAZUS typologies and depend on building construction type (wood, reinforced concrete, etc.) and the seismic code [67].

The present study explores three mitigation options for reducing the risk of earthquake and tsunami damage to buildings located in the Seaside region. The first option, referred to as Option 1, involves retrofitting the building to the highest seismic code. This option is assumed to improve the building's resistance to earthquake damage, but it is hypothesized to have no effect on the damage caused by tsunamis. The cost of retrofitting a building is estimated to be 30% of its market value. The second option, referred to as Option 2, involves relocating the building outside of the tsunami inundation zone.

296 Ea 297 re 298 ts 299 re 300 cc 301 is 302 th 303 m

Earthquake intensity measures for each recurrence interval are uniform throughout the Seaside, and we assume that relocated buildings are outside the inundation zone but within the city boundaries. As such, this option results in no tsunami damage while also having no effect on the earthquake intensity measures a building is subject to. The cost of relocating a building is estimated to be 100% of its market value. The final option, referred to as Option 3, involves a combination of both retrofitting and relocation. This option aims to mitigate both earthquake and tsunami damage and is hypothesized to be the most effective in reducing risk. The cost of implementing Option 3 is estimated to be 130% of the building's market value. It is important to note that these estimates are based on the assumptions and hypotheses mentioned above, and future research may reveal different results. The objective of this study is to explore the relative efficacy of these three mitigation options and to provide guidance for future risk reduction strategies in the Seaside region.

305

304

Table 2: Mitigation options available at each parcel

Option	Description	Targeted Hazard	Cost (%RMV)	
0	Do nothing (status quo)	-	-	
1	Retrofit structure to high-seismic code	Earthquake	30%	
2	Relocate structure	Tsunami	100%	
Relocate and retrofit to high-seismic code		Earthquake and Tsunami	130%	

306

307 308

309

312

313

314

315

316

317

318

319

320

Assuming these strategy costs based on the current retail value of the building, we can now quantify the expense of a mitigation strategy at the building stage. The cost of improving from mitigation option $k \in \mathcal{K}$ to mitigation option $k' \in \mathcal{K}$, in parcel $i \in \mathcal{Z}$ is $c_{ikk'}$ calculated following Equation (22).

$$c_{ikk'} = v_{ik} * w_{kk'} \tag{22}$$

Where, v_{ik} is the retail market value (also known as building appraisal value) of the building in parcel $i \in \mathcal{Z}$ and $w_{kk'}$ is cost percentage of v_{ik} to improve from mitigation option $k \in \mathcal{H}$ to mitigation option $k' \in \mathcal{H}$.

The present study evaluates the potential impact of three budget scenarios, with budget amounts of \$40 million, \$80 million, and \$120 million, on the community's overall economic loss, population dislocation, and repair times in two multi-hazard scenarios, namely the 500-year return period and the 1000-year return period. The evaluation is conducted at the building level, and the mitigation options analyzed include retrofitting buildings to the highest seismic code, relocating buildings outside of the tsunami inundation zone, and a combination of both retrofitting and relocation.

4. Results and Discussion

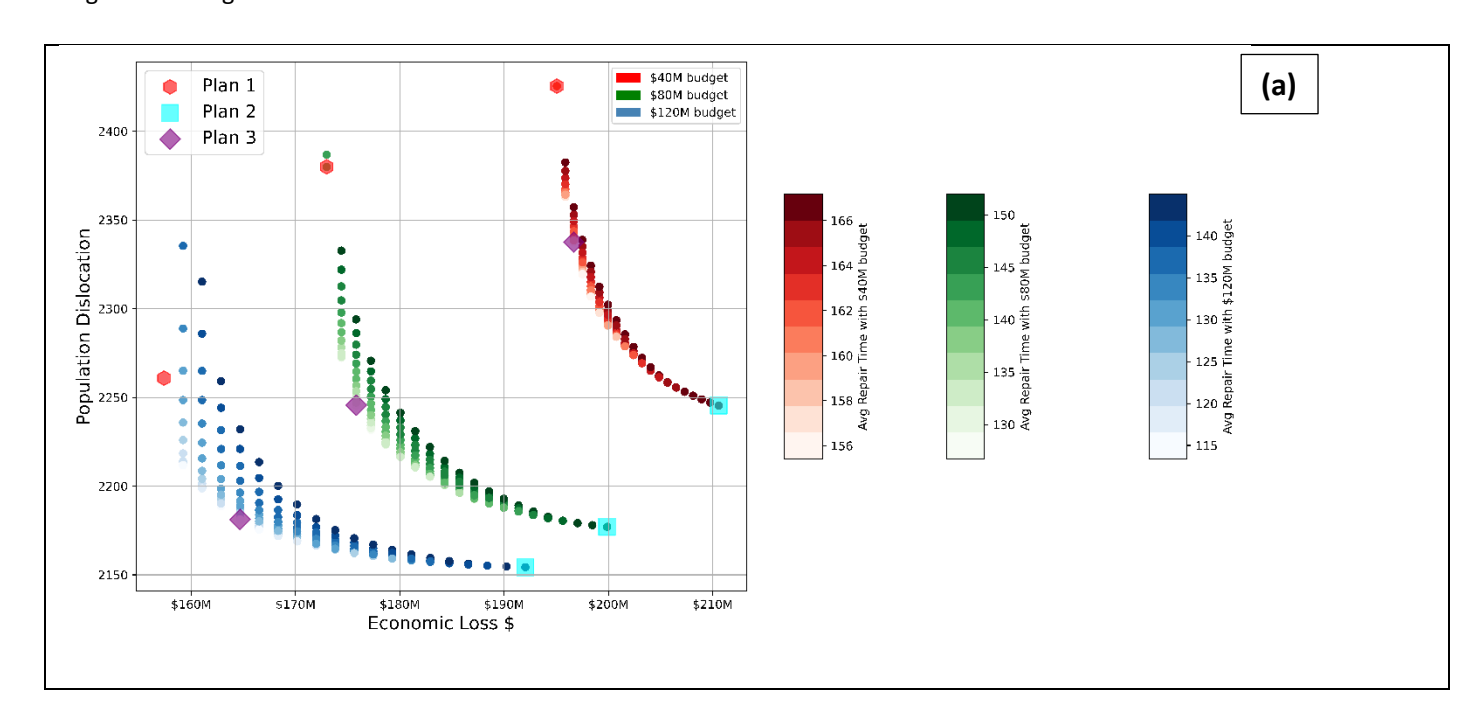
The ϵ -constraint approach was used to handle multi-objective optimization problem here where multiple objectives are in conflict with each other and there is no single solution that is optimal for all objectives [68,69]. The ϵ -constraint approach allows for the generation of a set of solutions, called the Pareto front, that are non-dominated by any other

solution. These solutions represent the trade-off between the conflicting objectives and allow decision makers to select a solution that is most suitable for their needs based on their specific priorities and constraints [70,71].

4.1. Analysis of Multi-hazard Mitigation

The results of the optimization model, using the ε-constraint approach, are presented in **Figures 4 (a) and (b)** and illustrate the trade-offs between direct economic loss, population dislocation, and average repair time. The solutions are shown on the Pareto front with different budget levels, with red, green, and blue representing solutions with budgets of \$40 million, \$80 million, and \$120 million, respectively. Three points are highlighted on each surface, known as Plan 1, Plan 2, and Plan 3, which represent the optimal solutions in terms of minimizing economic loss, population dislocation, and repair time. The results shown in **Figures 4 (a)** and **4 (b)** depict the outcomes for a 500-year and a 1000-year multi-hazard event, respectively. It is important to note that the repair time estimates presented are optimistic and previous studies have indicated that repair times may be longer when considering the broader regional context in which a community is located [56].

In the case study under consideration, a set of feasible strategies was evaluated, and three plans were selected for further analysis. These plans were characterized based on the direct economic damage they would cause, the population displacement they would result in, and the estimated repair times. By evaluating these trade-offs at different budget levels, a more comprehensive understanding of the relative merits of each strategy can be achieved. The results of this analysis can then inform the selection of the best course of action to prepare for the event. The results of the tradeoff analysis for three different budget levels (\$40 million, \$80 million, and \$120 million) are presented in **Table 3**, **Table 4**, and **Table 5** respectively. These tables provide insight into the balance between the three conflicting objective functions and the most cost-effective mitigation options available for each budget level. The results from the tradeoff analysis enable us to identify the trade-offs between the different objective functions and make informed decisions about the optimal mitigation strategies.



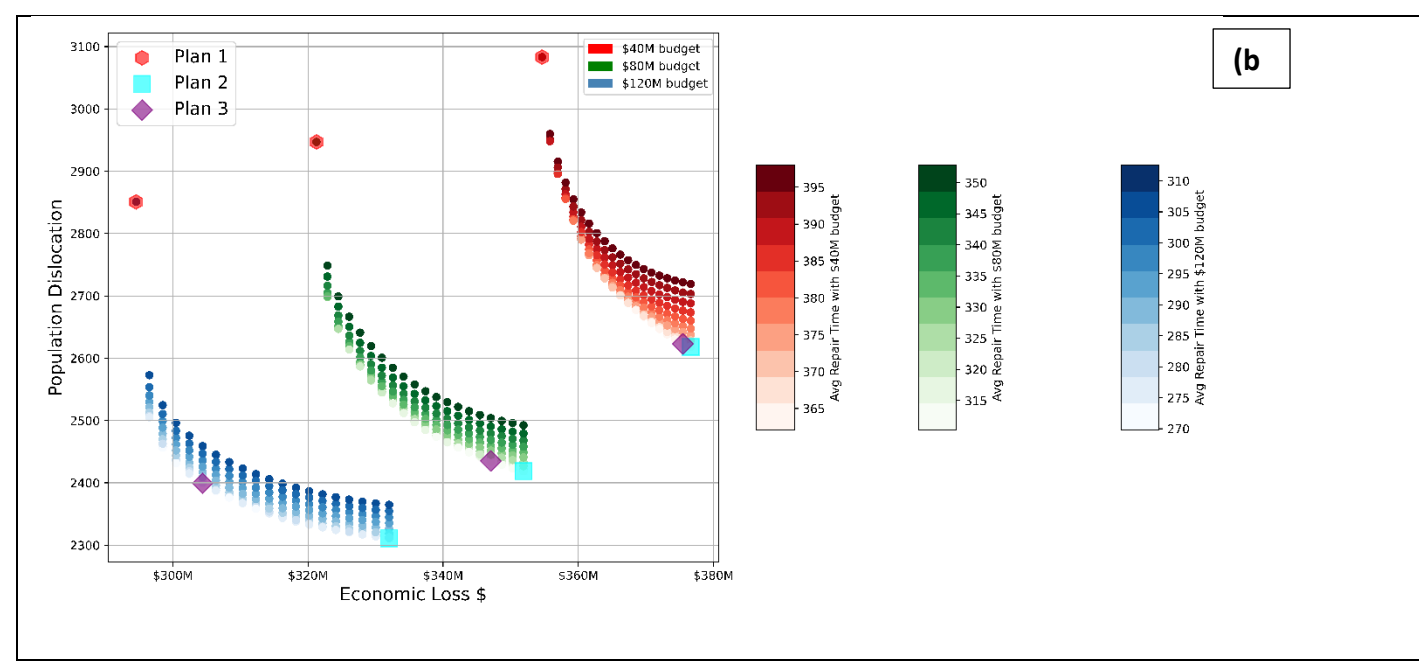


Figure 4: Relationship between economic loss and population dislocation for (a) 500-year event, and (b) 1000-year event

346

343

344

Table 3: Tradeoff Analysis between the objectives at \$40M budget

Plans	Economic loss	Population dislocation	Repair Time (Days)	Number of buildings not retrofitted	Number of buildings mitigated		
	(Million)				Option – 1	Option – 2	Option – 3
500 years	\$195	2425	162	3425	1028	0	0
(Plan 1)							
500 years (Plan 2)	\$210	2245	167	3005	1366	3	79
500 years	\$197	2338	155	3133	1306	5	6
(Plan 3)	\$355	3083	398	3840	613	0	0
(Plan 1) 1000 years	\$377	2618	363	3433	684	169	167
(Plan 2) 1000 years	\$375	2623	362	3420	706	187	140
(Plan 3)							

348

350

Table 5: Tradeoff Analysis between the objectives at \$120M budget

Plans	Economic loss (Million)	Population dislocation	Repair Time (Days)	Number of buildings not retrofitted	Number of buildings mitigated		
					Option – 1	Option – 2	Option – 3
500 years (Plan 1)	\$157	2261	116	1823	2565	10	55
500 years (Plan 2)	\$192	2154	145	2239	1746	4	465
500 years (Plan 3)	\$164	2181	113	1759	2453	20	221
1000 years (Plan 1)	\$295	2851	313	2808	1317	355	0
1000 years (Plan 2)	\$332	2311	279	2581	1042	136	694
1000 years (Plan 3)	\$304	2399	270	2412	1363	344	334

The choice of budget level is a crucial factor in determining the most appropriate strategy to be adopted in preparation for a hazard event. The aim of this study is to analyze the trade-off between different budget levels and the corresponding outcomes in terms of economic loss, population displacement, and repair time. For the selected case study, three plans were analyzed with varying budget levels. An analysis of the results for a 500-year event reveals that the minimum economic loss is achieved with Plan 1, with a return on investment of 105% for a budget of \$40 million. This budget level resulted in a reduction of economic loss from \$237 million to \$195 million. On the other hand, budget levels of \$80 million and \$120 million yield return of 80% and 66%, respectively. In terms of repair time, the \$40 million investment results in a 40% improvement, while the \$80 million and \$120 million investments yield improvements of 73% and 94%, respectively. It is important to note that the minimum population dislocation of 2245 households can be reduced by 121 households with an additional \$40 million investment, which also results in a reduction of \$61.6 million in direct economic

The tradeoffs are numerous, and the outcomes produced by the optimization model can be used in various analyses, allowing the decision-maker to choose the best plan for their community based on these insights. This model's capability ranges from providing an overall optimum value on how much we can save in economic loss, population dislocation, and repair times to informing the user which building needs to be retrofitted with which strategy to achieve these values within a variety of budgets.

loss.

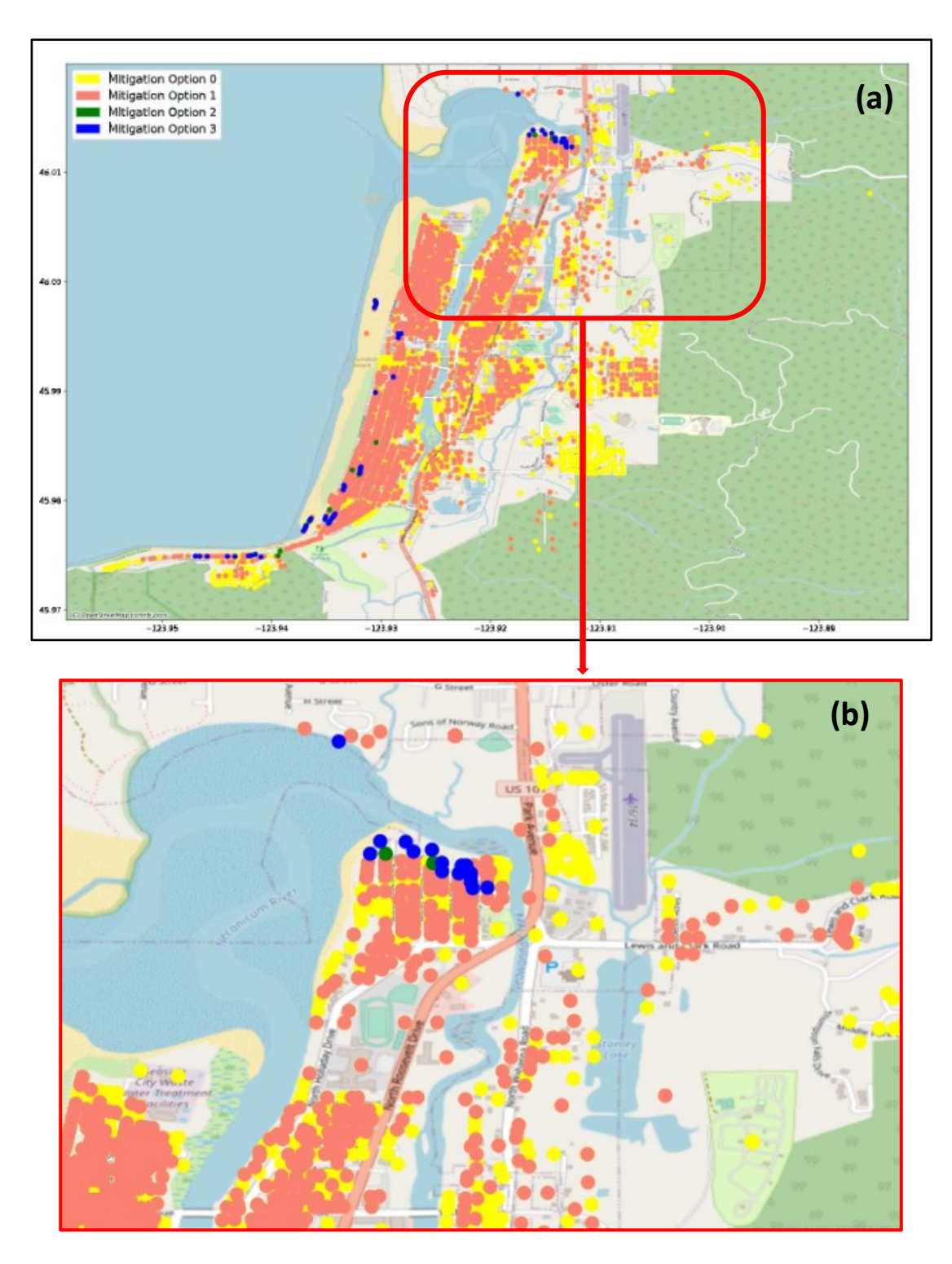


Figure 5: Example illustration of retrofitting plan – 1 for (a) a 500-year hazard for Seaside with \$120 M budget level, (b) detailed view of a certain location 500-year hazard for Seaside with \$120 M budget level

The results of the spatial analysis indicate the effectiveness of different mitigation strategies based on various budget levels and different objectives. As the budget increases, more structures are found to be optimal to retrofit to the highest seismic code, even if they need to be relocated. It is noteworthy that a few structures are only relocated without

379

380

381

retrofitting. The results show that the urban corridor of Seaside remains in its current state regardless of the budget level and objective, as it is not a residential area. However, the surrounding residential areas are either retrofitted or relocated.

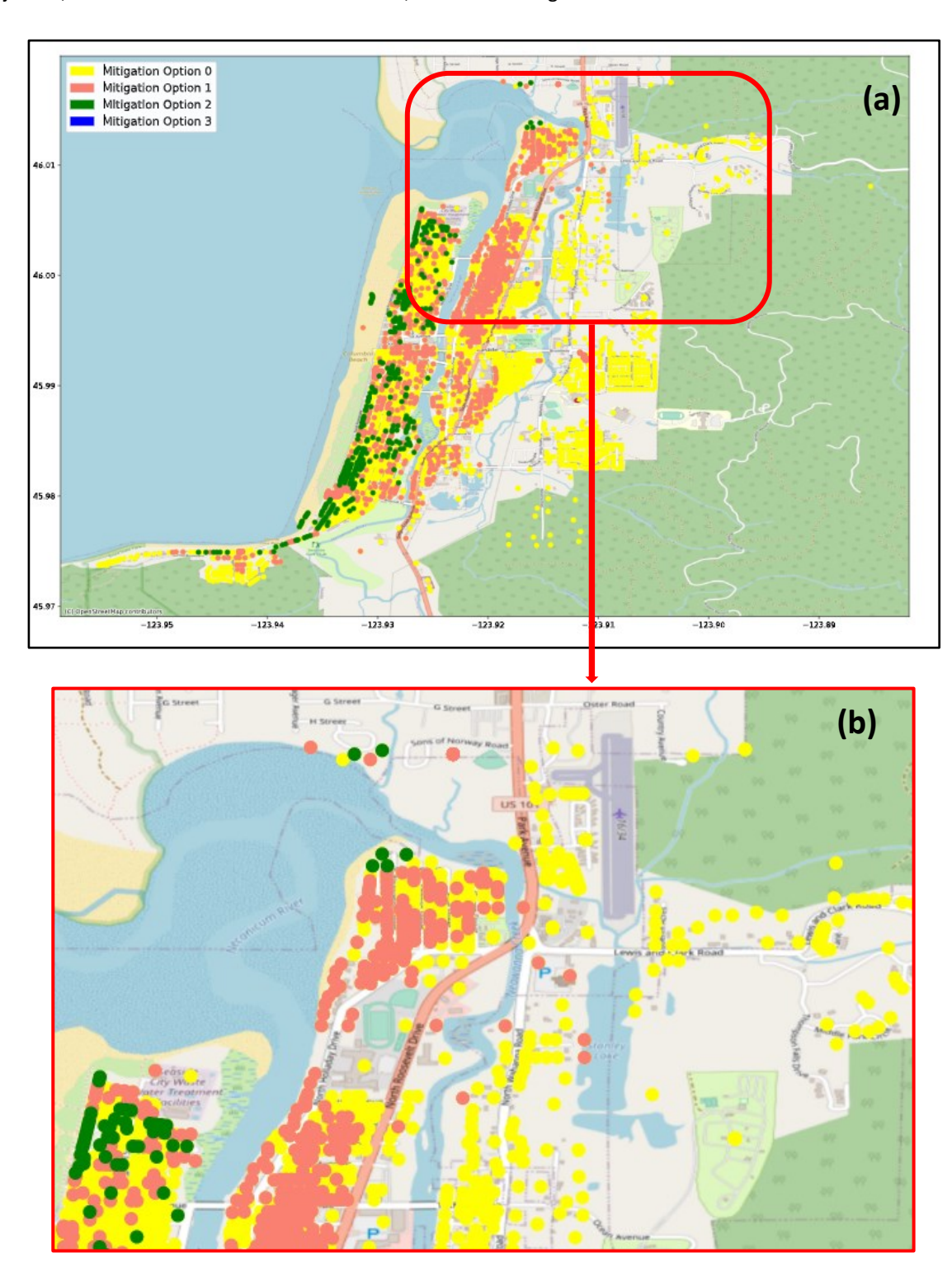


Figure 6: Example illustration of retrofitting plan – 1 for (a) a 1000-year hazard for Seaside with \$120 M budget level, (b) detailed view of a certain location 1000-year hazard for Seaside with \$120 M budget level

The analysis further reveals that with an increased recurrence interval of a natural hazard, such as a tsunami, a significant number of structures shift from retrofitting to relocating. The objective of minimizing economic losses results in the urban

corridor beginning to shift from its current state to either retrofitting or relocating. Figure 5 and Figure 6 provide an overview of the distribution of various mitigation measures. Figure 7 depicts Plan 1 on the top and Plan 2 on the bottom for the 500-year scenario with a \$40M budget. In Plan 1, where we have the least economic loss, the model selects the coastal area with mitigation strategy 1, which is the region with the most costly buildings used for seasonal and recreational use. The model's tendency to retrofit the most expensive buildings in order to incur the least economic loss demonstrates the model's preferences in terms of optimal tradeoffs. In Plan 2 Figure 7, we can see that the spread of strategies is even around the map to help get the least population dislocation while minimizing the total economic loss by proposing relocated buildings in coastal regions, i.e., mitigation strategy 3.

The transition in mitigation strategy visible in the three chosen plans represents the model's broader pattern of moving investments from residential to non-residential structures. When these are compared to the competing repair times, the decision maker gets a unique perspective.

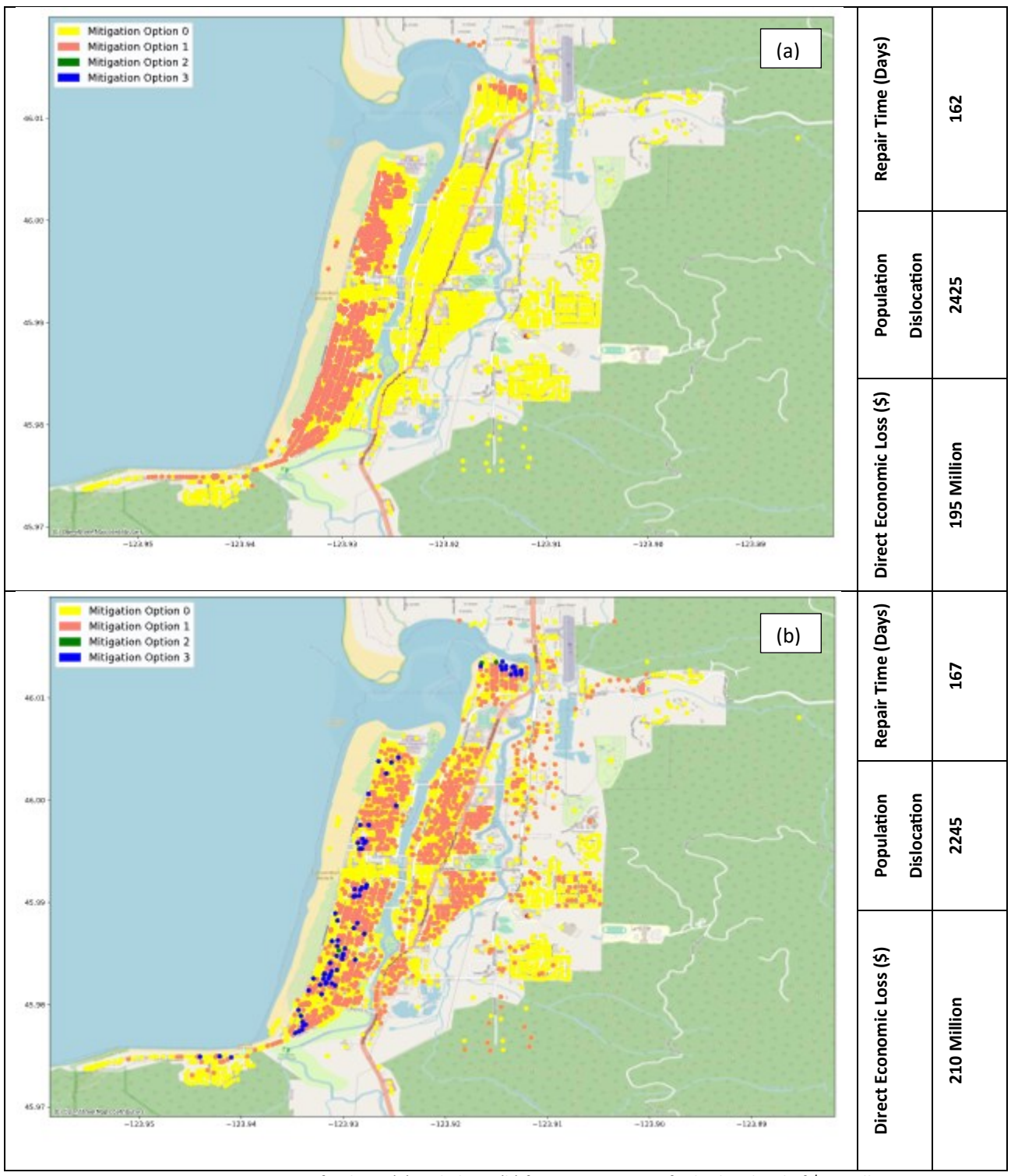


Figure 7: Comparing Retrofit Plan 1 (a) and Plan 2 (b) for 500-year Event for budget level of \$40 million.

4.2. Comparative Analysis of Seismic and Multi-hazard

412

413

414

415

416

417

In hazard and risk assessment, it's imperative to discern the distinct impacts of individual hazards as well as their combined effects. This section presents a detailed comparison between scenarios considering solely seismic hazard and those incorporating both seismic and tsunami hazards. This analytical approach allows for a clearer comprehension of the inherent complexities and potential compounded effects that can arise from multi-hazard scenarios. By differentiating

these scenarios, this section seeks to emphasize the significance and practical implications of a multi-hazard approach in engineering risk assessments, thereby reinforcing the key theme of "multiple hazards" within this study. As we mentioned earlier in this paper, Seaside, Oregon, located near the Cascadia Subduction Zone, is particularly vulnerable to both earthquakes and tsunamis [45,55,57,72,73]. This subduction zone, where the Juan de Fuca plate moves beneath the North American plate, has historically triggered significant seismic events. When stress accumulated between these plates is suddenly released, it not only causes an earthquake but also leads to the sudden displacement of the seabed. This underwater movement, in turn, can generate tsunamis, given the direct path between the origin of the seismic activity and Seaside's coastal location. This is why earthquakes and tsunamis are mostly concurrent unwanted events in Seaside.

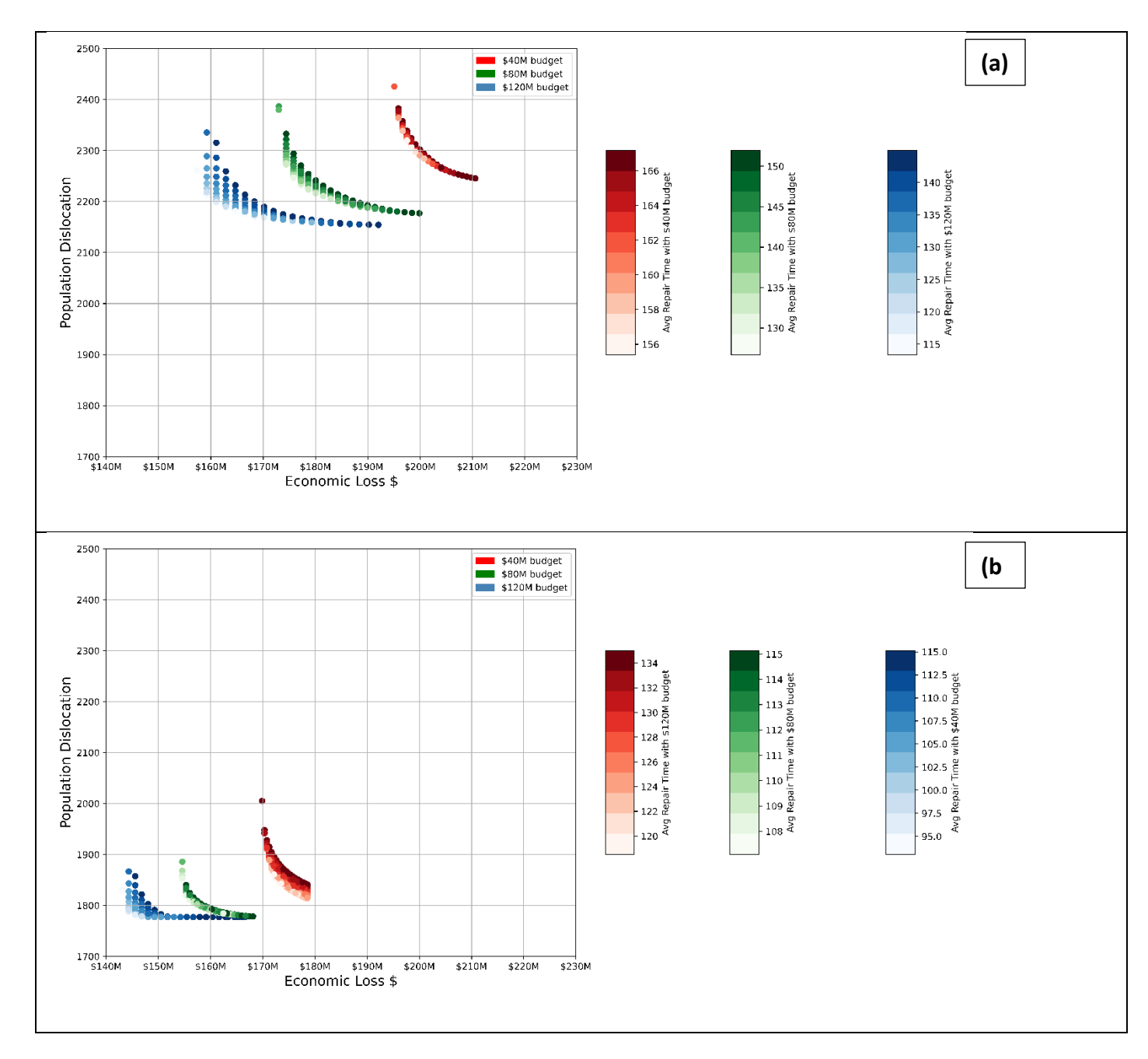


Figure 8: Comparative analysis of the multi-hazard scenario (a) with seismic hazard scenario (b) in various budget level

Figure 8 presents a comparative study of the scenario of multiple hazard and seismic hazard on Seaside, Oregon for a 500-year event. As this a multi-objective optimization problem, where are trying to minimize the total direct economic loss due to building damage, population dislocation, and average repair time of the building, after solving the problem we got multiple optimal solutions in the solution space. It will be then on the decision maker and based on his/her priority to trade off among objective functions to choose the correct plan. In the case of both seismic and multi-hazard scenario in the Figure 8, it is visible that the range of improvement in minimization of economic loss is low compared to the higher investment scenario as in higher budget level decision makers are getting more options to improve or retrofit building structures. However, as the buildings are getting impacted more in multi-hazard scenarios, population dislocation is higher in the case of this scenario compared to seismic hazard.

5. Conclusion

To effectively address the increasing threat of natural hazards, communities must prioritize resilience and preparedness measures. This study aimed to contribute to the development of resilient communities by presenting a novel multi-objective optimization model for building retrofit decision-making. This model can support building owners in their analysis of how investments in retrofit measures can impact community vulnerability. The study was implemented in Seaside, Oregon, a community subject to seismic-tsunami hazards associated with the Cascadia Subduction Zone. The e-constraint approach is used to generate a set of non-dominated solutions, known as the Pareto front, which allows for a trade-off analysis of the different mitigation options. The study evaluates three plans based on their economic loss, population dislocation, and repair time and presents the trade-offs between these objectives at different budget levels. The results of the study enable decision-makers to make informed decisions about the most cost-effective mitigation strategies for their community.

However, in this paper, we considered the uncertainty of the natural hazard in the prediction of model parameters as natural hazards are always uncertain, but it was not considered inside the optimization modeling techniques. In future work, it would be valuable to incorporate uncertainty into the current optimization model to improve its accuracy and applicability. Additionally, considering multiple layers of decision-making in the optimization model can further enhance its usefulness in real-world applications. This study presents an optimization framework for the optimal allocation of limited resources for building retrofitting and relocation. While the model assumes a centralized budget, we recognize that in real-world contexts, funding often comes from individual building owners. Furthermore, the proposed model could be used to depict a scenario where a centralized entity (say, the local government) is determining how to distribute budget between building owners, to subsidize their individual mitigation actions. Nonetheless, our model offers valuable insights that can guide community incentive programs or inform grant applications to federal agencies. Furthermore, while our model suggests optimal solutions under the assumption of a single, benevolent decision-maker, real-world implementation is far more complex. Decision-making processes involve multiple stakeholders, each with their own priorities and constraints. Local governments, community organizations, building owners, and residents all play crucial roles in such endeavors.

Furthermore, one of the pivotal assumptions in our model pertains to the retrofitting costs, which we initially set at 30% of the replacement value. This assumption, while illustrative, has significant implications for the outcomes of our model. For instance, if retrofitting costs were to increase, the economic constraints could potentially reduce the number of buildings recommended for retrofitting. It's essential to emphasize that the 30% figure, while based on certain industry standards and previous studies, is not universally applicable. Different regions, building types, and retrofitting techniques might have varying costs. Moreover, the complexity of the retrofitting process, the availability of materials and skilled labor, and the specific requirements of a building can all influence the final cost. The sensitivity of our model to this parameter underscores the importance of context-specific, accurate, and up-to-date cost estimates. While our model provides a foundational framework for understanding the trade-offs and benefits of retrofitting versus replacement, it's crucial for decision-makers to integrate local and current data to make informed decisions. In light of this, we recommend that future applications of this model incorporate a sensitivity analysis around retrofitting costs. This would allow stakeholders to understand the range of potential outcomes based on varying cost estimates. Furthermore, collaborating with industry experts and gathering empirical data can refine these assumptions, enhancing the model's applicability and robustness. The multi-objective formulation of the model presented herein allows decision-makers the ability to explore tradeoffs across different priorities. Single-objective models, such as those focused on minimizing economic losses, inherently prioritize retrofitting high-value properties. This is because these properties contribute more significantly to overall economic losses in the event of a disaster. While effective for loss reduction, this raises equity concerns, especially for vulnerable community members in lower-value properties. The multi-objective aspect allows decision-makers to explore solutions across competing priorities - e.g., minimize losses and population dislocation. This model can be expanded in future work to further explore equity by considering additional objective functions relevant to socioeconomic metrics, such as the social vulnerability index [21,74,75]. This will ensure a balanced and inclusive approach to disaster mitigation.

This study has made a significant contribution to the field of multi-hazard resilience and provides a valuable tool for decision-makers in their efforts to make communities more resilient to natural hazards. By considering multiple objective functions and presenting multiple retrofit plans, this model allows for a more comprehensive and data-driven approach to building retrofit decision-making. Although we studied our model effectiveness on physical infrastructure and economic parameters, the role of social capital in community resilience and disaster risk reduction is noteworthy and warrants further examination. Social capital can be considered an additional layer that contributes to a community's ability to prepare for, respond to, and recover from natural hazards. In future work, the optimization model could be expanded to integrate metrics related to social capital, such as community engagement, trust, and social networks [32,33]. The model can be applied to other communities and serves as a starting point for further research and development in the field of building resilience and disaster preparedness.

Data Availability Statement

463

464

465

466

467

468

469

470

471

472

473

474

475

476

477

478

479

480

481

482

483

484

485

486

487

488

489

490

491

492

493

494

495

496

497

The data presented in this study are available in the Interdependent Networked Community Resilience Modeling Environment (INCORE) [59,76] and also on request from the corresponding author.

498 Funding

504

505

506

507

508

509

510

511

512

513

514

This research received funding from prestigious organizations committed to advancing science. The National Institute of Standards and Technology (NIST) Center of Excellence for Risk-Based Community Resilience Planning provided partial support for this study through a cooperative agreement with Colorado State University. The NIST funding was identified by grant numbers 70NANB20H008 and 70NANB15H044. Additionally, the National Science Foundation (NSF) contributed to this research through award number 2052930.

Acknowledgment

We would like to acknowledge that the views and opinions expressed in this research paper are solely those of the authors and do not necessarily reflect the official stances or perspectives of the esteemed National Institute of Standards and Technology (NIST) or the National Science Foundation (NSF). While we greatly appreciate the support and funding provided by these organizations, we take full responsibility for the content presented in this paper. We remain deeply committed to the principles of academic integrity and intellectual independence and express our sincere gratitude to NIST and NSF for their unwavering commitment to advancing scientific knowledge and research excellence. We would also like to extend our gratitude to the National Center for Supercomputing Applications (NCSA) and Interdependent Networked Community Resilience Modeling Environment (INCORE) for their invaluable support in providing data for the Seaside, Oregon, which significantly contributed to this study.

Conflict of Interest

The authors declare no conflict of interest.

516 References

- 517 [1] M. Koliou, J.W. van de Lindt, T.P. McAllister, B.R. Ellingwood, M. Dillard, H. Cutler, State of the research in community resilience: progress and challenges, Sustain Resilient Infrastruct. 5 (2020) 131–151. https://doi.org/10.1080/23789689.2017.1418547.
- 520 [2] M.S. Kappes, M. Keiler, K. von Elverfeldt, T. Glade, Challenges of analyzing multi-hazard risk: A review, Natural Hazards. 64 (2012) 1925–1958. https://doi.org/10.1007/s11069-012-0294-2.
- 522 [3] Y. Almoghathawi, A.D. González, K. Barker, Exploring Recovery Strategies for Optimal Interdependent Infrastructure Network Resilience, Netw Spat Econ. (2021). https://doi.org/10.1007/s11067-020-09515-4.
- M. Savari, H. Eskandari Damaneh, H. Eskandari Damaneh, The effect of social capital in mitigating drought impacts and improving livability of Iranian rural households, International Journal of Disaster Risk Reduction. 89 (2023) 103630. https://doi.org/10.1016/J.IJDRR.2023.103630.
- 527 [5] M.A. Meyer, Social Capital in Disaster Research, Handbooks of Sociology and Social Research. (2018) 263–286. 528 https://doi.org/10.1007/978-3-319-63254-4_14/COVER.
- 529 [6] R.B. Bhandari, Social capital in disaster risk management; a case study of social capital mobilization following the
 530 1934 Kathmandu valley earthquake in Nepal, Disaster Prevention and Management: An International Journal. 23
 531 (2014) 314–328. https://doi.org/10.1108/DPM-06-2013-0105/FULL/PDF.

- 532 [7] S. Sanyal, J.K. Routray, Social capital for disaster risk reduction and management with empirical evidences from Sundarbans of India, International Journal of Disaster Risk Reduction. 19 (2016) 101–111. https://doi.org/10.1016/J.IJDRR.2016.08.010.
- J.K. Behera, Role of social capital in disaster risk management: a theoretical perspective in special reference to Odisha, India, International Journal of Environmental Science and Technology. 20 (2023) 3385–3394. https://doi.org/10.1007/S13762-021-03735-Y/FIGURES/2.
- 538 [9] S.L.; Cutter, C.T. Emrich, J.T.; Mitchell, B.J. Boruff, The Long Road Home: Race, Class, and Recovery from Hurricane Katrina, 2006.
- 540 [10] R. Costa, T. Haukaas, S.E. Chang, Agent-based model for post-earthquake housing recovery, Earthquake Spectra. 37 (2021) 46–72. https://doi.org/10.1177/8755293020944175.
- 542 [11] S. Nozhati, B.R. Ellingwood, E.K.P. Chong, Stochastic optimal control methodologies in risk-informed community resilience planning, Structural Safety. 84 (2020) 101920. https://doi.org/10.1016/j.strusafe.2019.101920.
- J.D. Goltz, K. Yamori, Tsunami Preparedness and Mitigation Strategies, Oxford Research Encyclopedia of Natural Hazard Science. (2020). https://doi.org/10.1093/ACREFORE/9780199389407.013.324.
- 546 [13] O.M. Nofal, J.W. van de Lindt, H. Cutler, M. Shields, K. Crofton, Modeling the impact of building-level flood mitigation measures made possible by early flood warnings on community-level flood loss reduction, Buildings. 11 (2021). https://doi.org/10.3390/buildings11100475.
- P. Shane Crawford, J. Mitrani-Reiser, E.J. Sutley, T.Q. Do, T. Tomiczek, O.M. Nofal, J.M. Weigand, M. Watson, J.W. van de Lindt, A.J. Graettinger, Measurement Approach to Develop Flood-Based Damage Fragilities for Residential Buildings Following Repeat Inundation Events, ASCE ASME J Risk Uncertain Eng Syst A Civ Eng. 8 (2022). https://doi.org/10.1061/ajrua6.0001219.
- 553 [15] E.J. Sutley, J.W. van de Lindt, L. Peek, Community-Level Framework for Seismic Resilience. II: Multiobjective 554 Optimization and Illustrative Examples, Nat Hazards Rev. 18 (2017)04016015. 555 https://doi.org/10.1061/(asce)nh.1527-6996.0000230.
- 556 [16] F. Berkes, H. Ross, Community Resilience: Toward an Integrated Approach, Soc Nat Resour. 26 (2013) 5–20. https://doi.org/10.1080/08941920.2012.736605.
- 558 [17] M. Bruneau, S.E. Chang, R.T. Eguchi, G.C. Lee, T.D. O'Rourke, A.M. Reinhorn, M. Shinozuka, K. Tierney, W.A. Wallace, D. Von Winterfeldt, A Framework to Quantitatively Assess and Enhance the Seismic Resilience of Communities, Earthquake Spectra. 19 (2003) 733–752. https://doi.org/10.1193/1.1623497.
- 561 [18] S. Hosseini, K. Barker, J.E. Ramirez-Marquez, A review of definitions and measures of system resilience, Reliab Eng Syst Saf. 145 (2016) 47–61. https://doi.org/10.1016/j.ress.2015.08.006.
- 563 [19] C.D. Nicholson, K. Barker, J.E. Ramirez-Marquez, Flow-based vulnerability measures for network component 564 importance: Experimentation with preparedness planning, Reliab Eng Syst Saf. 145 (2015) 62–73. 565 https://doi.org/10.1016/j.ress.2015.08.014.
- D. Gama Dessavre, J.E. Ramirez-Marquez, K. Barker, Multidimensional approach to complex system resilience analysis, Reliab Eng Syst Saf. 149 (2016) 34–43. https://doi.org/10.1016/j.ress.2015.12.009.
- 568 [21] D.B. Karakoc, Y. Almoghathawi, K. Barker, A.D. González, S. Mohebbi, Community resilience-driven restoration 569 model for interdependent infrastructure networks, International Journal of Disaster Risk Reduction. 38 (2019) 570 101228. https://doi.org/10.1016/J.IJDRR.2019.101228.

- 571 [22] H. Baroud, K. Barker, J.E. Ramirez-Marquez, C.M. Rocco S., Importance measures for inland waterway network resilience, Transp Res E Logist Transp Rev. 62 (2014) 55–67. https://doi.org/10.1016/j.tre.2013.11.010.
- From R. Guidotti, P. Gardoni, N. Rosenheim, Integration of physical infrastructure and social systems in communities' reliability and resilience analysis, Reliab Eng Syst Saf. 185 (2019) 476–492. https://doi.org/10.1016/j.ress.2019.01.008.
- P. Franchin, F. Cavalieri, Probabilistic assessment of civil infrastructure resilience to earthquakes, Computer-Aided Civil and Infrastructure Engineering. 30 (2015) 583–600. https://doi.org/10.1111/mice.12092.
- 8.5. Friedman, E.A. Law, N.J. Bennett, I. Kavvada, S. Moura

 7. A. Horvath

 7. Aligning sustainability and regional earthquake hazard mitigation planning: integrating greenhouse gas emissions and vertical equity, Environmental Research: Infrastructure and Sustainability. 2 (2022) 045013. https://doi.org/10.1088/2634-4505/ACA9F3.
- 581 [26] S. Thacker, D. Adshead, M. Fay, S. Hallegatte, M. Harvey, H. Meller, N. O'Regan, J. Rozenberg, G. Watkins, J.W. Hall, 1982 Infrastructure for sustainable development, Nature Sustainability 2019 2:4. 2 (2019) 324–331. https://doi.org/10.1038/s41893-019-0256-8.
- G. Shokry, I. Anguelovski, J.J.T. Connolly, (Mis-)belonging to the climate-resilient city: Making place in multi-risk communities of racialized urban America, J Urban Aff. (2023). https://doi.org/10.1080/07352166.2022.2160339.
- 586 [28] R.A. Davidson, J. Kendra, B. Ewing, L.K. Nozick, K. Starbird, Z. Cox, M. Leon-Corwin, Managing disaster risk 587 associated with critical infrastructure systems: a system-level conceptual framework for research and policy 588 guidance, Civil Engineering and Environmental Systems. 39 (2022)123-143. 589 https://doi.org/10.1080/10286608.2022.2067848.
- 590 [29] J. Koopman, Subawe, traditional knowledge, and faith-based organisations promoting social capital and disaster preparedness: A Lombok, Indonesia case study, International Journal of Disaster Risk Reduction. 94 (2023) 103837. https://doi.org/10.1016/J.IJDRR.2023.103837.
- 593 [30] J. Tasic, S. Amir, Informational capital and disaster resilience: the case of Jalin Merapi, Disaster Prev Manag. 25 (2016) 395–411. https://doi.org/10.1108/DPM-07-2015-0163/FULL/PDF.
- 595 [31] A. Tammar, S.S. Abosuliman, K.R. Rahaman, Social Capital and Disaster Resilience Nexus: A Study of Flash Flood 596 Recovery in Jeddah City, Sustainability 2020, Vol. 12, Page 4668. 12 (2020) 4668. 597 https://doi.org/10.3390/SU12114668.
- 598 [32] B. Pfefferbaum, R.L. Van Horn, R.L. Pfefferbaum, A Conceptual Framework to Enhance Community Resilience
 599 Using Social Capital, Clin Soc Work J. 45 (2017) 102–110. https://doi.org/10.1007/S10615-015-0556-Z/METRICS.
- 600 [33] C. Zeballos-Velarde, C. Butron-Revilla, G. Manchego-Huaquipaco, C. Yory, The role of ancestral practices as social capital to enhance community disaster resilience. The case of the Colca Valley, Peru, International Journal of Disaster Risk Reduction. 92 (2023) 103737. https://doi.org/10.1016/J.IJDRR.2023.103737.
- J.P. Newman, H.R. Maier, G.A. Riddell, A.C. Zecchin, J.E. Daniell, A.M. Schaefer, H. van Delden, B. Khazai, M.J. O'Flaherty, C.P. Newland, Review of literature on decision support systems for natural hazard risk reduction: Current status and future research directions, Environmental Modelling and Software. 96 (2017) 378–409. https://doi.org/10.1016/j.envsoft.2017.06.042.
- 607 S. Kameshwar, D.T. Cox, A.R. Barbosa, K. Farokhnia, H. Park, M.S. Alam, J.W. van de Lindt, Probabilistic decision-608 support framework for community resilience: Incorporating multi-hazards, infrastructure interdependencies, and 609 resilience in Bayesian network, Reliab Eng Saf. 191 (2019).goals Syst 610 https://doi.org/10.1016/j.ress.2019.106568.

- 611 [36] D.M. Frangopol, D.M. Asce, P. Bocchini, M. Asce, Resilience as Optimization Criterion for the Rehabilitation of Bridges Belonging to a Transportation Network Subject to Earthquake, 2011.
- 613 [37] C. Gomez, J.W. Baker, An optimization-based decision support framework for coupled pre- and post-earthquake infrastructure risk management, Structural Safety. 77 (2019) 1–9. https://doi.org/10.1016/j.strusafe.2018.10.002.
- 615 [38] W. Zhang, C. Nicholson, A multi-objective optimization model for retrofit strategies to mitigate direct economic 616 loss and population dislocation, Sustain Resilient Infrastruct. 1 (2016) 123–136. 617 https://doi.org/10.1080/23789689.2016.1254995.
- Fig. 139 Y. Wen, Development of Multi-objective Optimization Model of Community Resilience on Mitigation Planning, Doctoral Dissertation, University of Oklahoma, 2021.
- 620 [40] H. Sen Gupta, O.M. Nofal, A.D. González, C.D. Nicholson, J.W. van de Lindt, Optimal Selection of Short- and Long-621 Term Mitigation Strategies for Buildings within Communities under Flooding Hazard, Sustainability. 14 (2022) 622 9812. https://doi.org/10.3390/su14169812.
- 623 [41] A.D. González, L. Dueñas-Osorio, M. Sánchez-Silva, A.L. Medaglia, The Interdependent Network Design Problem 624 for Optimal Infrastructure System Restoration, Computer-Aided Civil and Infrastructure Engineering. 31 (2016) 625 334–350. https://doi.org/10.1111/MICE.12171.
- W. Zhang, N. Wang, C. Nicholson, Resilience-based post-disaster recovery strategies for road-bridge networks,
 Structure and Infrastructure Engineering. 13 (2017) 1404–1413.
 https://doi.org/10.1080/15732479.2016.1271813.
- [43] H. Sen Gupta, Optimal Selection of Short- and Long-term Mitigation Strategies for Flooding Hazards, Master's
 Thesis, University of Oklahoma, 2022.
- 631 [44] F. Nhrap, Hazus Tsunami Model Technical Manual Hazus 4.2 Service Pack 3, (2021).
- H. Park, M.S. Alam, D.T. Cox, A.R. Barbosa, J.W. van de Lindt, Probabilistic seismic and tsunami damage analysis (PSTDA) of the Cascadia Subduction Zone applied to Seaside, Oregon, International Journal of Disaster Risk Reduction. 35 (2019). https://doi.org/10.1016/j.ijdrr.2019.101076.
- 635 [46] R.P. Clarke, Natural disaster mitigation using advanced ferrocement - Future research directions for improved 636 building resilience, Case Studies in Construction Materials. 16 (2022)e00990. 637 https://doi.org/10.1016/J.CSCM.2022.E00990.
- N. Rosenheim, R. Guidotti, P. Gardoni, W.G. Peacock, Integration of detailed household and housing unit characteristic data with critical infrastructure for post-hazard resilience modeling, Sustain Resilient Infrastruct. 6 (2021) 385–401. https://doi.org/10.1080/23789689.2019.1681821.
- J.-W. Bai, M. Beth, D. Hueste, P. Gardoni, J.-W. Bai[^], D. Hueste[^], P. Gardonf, E.B. Snead, Probabilistic Assessment
 of Structural Seismic Damage for Buildings in Mid-America, AIP Conf Proc. 1020 (2008) 1685.
 https://doi.org/10.1063/1.2963799.
- 644 [49] Y.-S. Lin, W. Gillis Peacock, J.-C. Lu, Y. Zhang, Dislocation Algorithm 3-Logistic Regression Approach, 2008.
- 645 [50] M. Koliou, J.W. van de Lindt, Development of Building Restoration Functions for Use in Community Recovery 646 Planning to Tornadoes, Nat Hazards Rev. 21 (2020) 04020004. https://doi.org/10.1061/(asce)nh.1527-647 6996.0000361.
- C. Goldfinger, C. Hans Nelson, A.E. Morey, J.E. Johnson, J.R. Patton, E. Karabanov, J. Gutiérrez-Pastor, A.T. Eriksson,
 E. Gràcia, G. Dunhill, R.J. Enkin, A. Dallimore, T. Vallier, Turbidite Event History-Methods and Implications for
 Holocene Paleoseismicity of the Cascadia Subduction Zone, n.d.

- N. Wood, Scientific Investigations Report 2007-5283 Variations in City Exposure and Sensitivity to Tsunami Hazards in Oregon, n.d.
- 653 [53] H. Park, D.T. Cox, A.R. Barbosa, Comparison of inundation depth and momentum flux based fragilities for probabilistic tsunami damage assessment and uncertainty analysis, Coastal Engineering. 122 (2017) 10–26. https://doi.org/10.1016/j.coastaleng.2017.01.008.
- D. Sanderson, D. Cox, G. Naraharisetty, A spatially explicit decision support framework for parcel- and community-level resilience assessment using Bayesian networks, Sustain Resilient Infrastruct. 7 (2022) 531–551. https://doi.org/10.1080/23789689.2021.1966164.
- D. Sanderson, S. Kameshwar, N. Rosenheim, D. Cox, Deaggregation of multi-hazard damages, losses, risks, and connectivity: an application to the joint seismic-tsunami hazard at Seaside, Oregon, Natural Hazards. 109 (2021) 1821–1847. https://doi.org/10.1007/S11069-021-04900-9.
- D. Sanderson, S.M. Asce, D. Cox, M. Asce, A.R. Barbosa, A.M. Asce, J. Bolte, Modeling Regional and Local Resilience
 of Infrastructure Networks Following Disruptions from Natural Hazards, Journal of Infrastructure Systems. 28
 (2022). https://doi.org/10.1061/(ASCE)IS.1943-555X.0000694.
- D.M. Wiebe, D.T. Cox, Application of fragility curves to estimate building damage and economic loss at a community scale: A case study of Seaside, Oregon, Natural Hazards. 71 (2014) 2043–2061. https://doi.org/10.1007/s11069-013-0995-1.
- 668 [58] M.T. Schultz, B.P. Gouldby, J.D. Simm, J.L. Wibowo, Beyond the factor of safety developing fragility curves to characterize system reliability, This Digital Resource Was Created in Microsoft Word and Adobe Acrobat. (2010). https://erdc-library.erdc.dren.mil/jspui/handle/11681/4766 (accessed February 11, 2023).
- [59] D. Cox, A. Barbosa, M. Alam, M. Amini, S. Kameshwar, H. Park, D. Sanderson, Report, in Seaside Testbed Data
 Inventory for Infrastructure, Population, and Earthquake-Tsunami Hazard, (2022). https://doi.org/10.17603/DS2 SP99-XV89.
- 674 J.W. van de Lindt, J. Kruse, D.T. Cox, P. Gardoni, J.S. Lee, J. Padgett, T.P. McAllister, A. Barbosa, H. Cutler, S. Van 675 Zandt, N. Rosenheim, C.M. Navarro, E. Sutley, S. Hamideh, The interdependent networked community resilience 676 modeling environment (IN-CORE), Resilient Cities and Structures. (2023)57-66. 677 https://doi.org/10.1016/J.RCNS.2023.07.004.
- 678 [61] J.W. van de Lindt, B. Ellingwood, T.P. McAllister, P. Gardoni, D. Cox, W.G. Peacock, H. Cutler, M. Dillard, J. Lee, L. 679 Peek, J. Mitrani-Reiser, Modeling Community Resilience: Update on the Center for Risk-Based Community 680 Resilience Planning and the Computational Environment IN-CORE, (2018).681 https://www.nist.gov/publications/modeling-community-resilience-update-center-risk-based-community-682 resilience-planning (accessed September 6, 2023).
- 683 [62] pylncore modules pylncore 1.8.0 documentation, (2023). https://incore.ncsa.illinois.edu/doc/pyincore/index.html (accessed February 11, 2023).
- J.W. Van De Lindt, J. Kruse, D.T. Cox, P. Gardoni, J.S. Lee, J. Padgett, T.P. Mcallister, A. Barbosa, H. Cutler, S. Van Zandt, Next Generation Resilience Community-Level Modeling: The Interdependent Networked Community Resilience Modeling Environment (IN-CORE), in: 14th International Conference on Applications of Statistics and Probability in Civil Engineering, ICASP14, 2023: pp. 1–10.
- 689 [64] P. Gardoni, J.W. van de Lindt, B.R. Ellingwood, T. McAllister, J.S. Lee, H. Cutler, W.G. Peacock, D. Cox, The
 690 Interdependent Networked Community Resilience Modeling Environment, Proceedings of the 16th European
 691 Conference on Earthquake Engineering. (2018) 1–10.

- 692 [65] Hazus Earthquake Model Technical Manual Hazus 4.2 SP3, (2020).
- 693 [66] Salem, The Oregon Resilience Plan Reducing Risk and Improving Recovery for the Next Cascadia Earthquake and
 694 Tsunami Report to the 77 th Legisla ve Assembly from Oregon Seismic Safety Policy Advisory Commission
 695 (OSSPAC), (2013).
- 696 [67] H. Park, D.T. Cox, M.S. Alam, A.R. Barbosa, Probabilistic seismic and tsunami hazard analysis conditioned on a 697 megathrust rupture of the cascadia subduction zone, Front Built Environ. 3 (2017). 698 https://doi.org/10.3389/fbuil.2017.00032.
- 699 [68] S. Bandaru, K. Deb, Multi-Objective Optimization, Decision Sciences. (2016) 161–200. 700 https://doi.org/10.1201/9781315183176-12.
- 701 [69] N. Gunantara, A review of multi-objective optimization: Methods and its applications, Cogent Eng. 5 (2018) 1–16. 702 https://doi.org/10.1080/23311916.2018.1502242.
- 703 [70] Y. Du, L. Xie, J. Liu, Y. Wang, Y. Xu, S. Wang, Multi-objective optimization of reverse osmosis networks by lexicographic optimization and augmented epsilon constraint method, Desalination. 333 (2014) 66–81. https://doi.org/10.1016/J.DESAL.2013.10.028.
- 706 [71] A review of multi-objective Gunantara, optimization: Methods and its applications, 707 Http://Www.Editorialmanager.Com/Cogenteng. 5 (2018)1-16. 708 https://doi.org/10.1080/23311916.2018.1502242.
- 709 [72] D.T. Cox, H. Park, M.S. Alam, A.R. Barbosa, Probabilistic tsunami hazard assessment and damage estimation of the
 710 built environment: Application to the Cascadia Subduction Zone and Seaside, Oregon, Proceedings of the Coastal
 711 Engineering Conference. 36 (2018) 2017.
- 712 [73] H. Park, D.T. Cox, Probabilistic assessment of near-field tsunami hazards: Inundation depth, velocity, momentum flux, arrival time, and duration applied to Seaside, Oregon, Coastal Engineering. 117 (2016) 79–96. https://doi.org/10.1016/j.coastaleng.2016.07.011.
- 715 [74] B.E. Flanagan, E.W. Gregory, E.J. Hallisey, J.L. Heitgerd, B. Lewis, A Social Vulnerability Index for Disaster Management, J Homel Secur Emerg Manag. 8 (2020). https://doi.org/10.2202/1547-717 7355.1792/MACHINEREADABLECITATION/RIS.
- 718 [75] K. Bergstrand, B. Mayer, B. Brumback, Y. Zhang, Assessing the Relationship Between Social Vulnerability and Community Resilience to Hazards, Soc Indic Res. 122 (2015) 391–409. https://doi.org/10.1007/S11205-014-0698-3/TABLES/2.
- 721 [76] IN-CORE, (2023). https://incore.ncsa.illinois.edu/login?origin=DataViewer (accessed March 2, 2023).

723